Mn(Ⅱ)

Solvent Control over Structural Diversity of Two Manganese Complexes Based on Furan-2 5-dicaboxylate

CHEN Wen-Xian   WU Geng-Huang   ZHUANG Gui-Lin   KONG Xiang-Jian[*]
LONG La-Sheng[*]   HUANG Rong-Bin   ZHENG Lan-Sun

（*State Key Laboratory of Physical Chemistry of Solid Surface Department of Chemistry*
College of Chemistry and Chemical Engineering Xiamen University Xiamen 361005 *China*）

Abstract   Two complexes namely Mn（FDC）（H₂O）₃(**1**) and H₂N（CH₃）₂₂・ Mn₃（FDC）₄ ・2DMF・H₂O (**2**)（H₂FDC = Furan-2 5-dicarboxylic acid） were synthesized *via* the solvothermal reaction of manganese（Ⅱ） chloride and furan-2 5-dicarboxylate acid under different solvent conditions. Single-crystal analysis reveals that one-dimensional complex **1** was obtained when the reaction was carried out in DMF/H₂O while three-dimensional complex **2** was synthesized when the reaction was carried out in DMF. Variable-temperature magnetic measurements and Quantum Monte Carlo（QMC） simulation indicate that both the complexes exhibit antiferromagnetic characteristic.
Keywords   Solvent effect; Metal-organic framework; Magnetism

The design and assembly of various coordination polymers with desired properties are currently of great interest due to their applications in fluorescence electricity magnetism and so on [1—16]. Generally coordination polymers were mainly assembled *via* the different types of intermolecular interactions such as metal-ligand complexation hydrogen bonding $\pi\cdots\pi$ halogen···halogen Au···Au and ionic interactions [17—20]. Compared to those of the covalent bonds the intermolecular interaction energies are relatively low which makes the assembly of coordination polymers very sensitive to external physical or chemical stimuli such as temperature

pH reaction time and reactants ratio [21—32]. Accordingly a detailed understanding of the role of external physical or chemical stimuli in the assembly of coordination polymers remains to be one of the most important fields in crystal engineering. Although great efforts have been focused on understanding the influences of pH value on the design of various carboxylate-based polymers [33—37] the investigation of solvent effect on the structures of coordination polymers remains scarce [38—44].

In this work we chose Mn/Furan-2 5-dicarboxylic acid(H_2FDC) system to investigate the effect of solvent on the assembly of coordination polymers based on the following considerations: as the multifunctional bridging dicarboxylic acid H_2FDC ligand should be able to form a varity of multi-dimensional coordiantion polymer although so far none has been reported; the manganese complexes with dicarboxylic acid ligands may display interesting magnetic properties similar to previous Mn-dicarboxylic complexes [45—47]. Herein lie the syntheses crystal structures and magnetic properties of two manganese(II) complexes Mn(FDC)(H_2O)$_3$ (**1**) and H_2N(CH$_3$)$_2$ $_2$· Mn$_3$(FDC)$_4$ · 2DMF · H_2O(**2**).

1 Experimental

1.1 Materials and Methods

All chemicals and solvents used in the syntheses were analytical grade and used without further purification. Infrared spectra were recorded with a Nicolet AVATAR FTIR360 spectrometer *via* the KBr pellet technique. Elemental analysis was carried out on a CE instruments EA 1110 elemental analyzer. The thermogravimetric analysis(TGA) was performed with a NETZSCH STA 449C instrument. Magnetic susceptibility was measured on a Quantum Design MPMS superconducting quantum interference device(SQUID).

1.2 Synthesis

1.2.1 Mn(FDC)(H_2O)$_3$(**1**)

Furan-2 5-dicarboxylic acid(H_2FDC 0.0156 g 0.1 mmol) and MnCl$_2$ · 4H_2O(0.0198 g 0.1 mmol) were dissolved in a mixture of DMF(1.0 mL) and H_2O(1.0 mL) with stirring at room temperature. When the pH value of the mixture was adjusted to about 4 with an ammonia solution and the solution(about 2.1 mL) was placed in a 10 mL conical flask. The container was heated to 100 ℃ at a rate of 5 ℃/min and kept at 100 ℃ for 24 h then slowly cooled down to room temperature at a rate of 3 ℃/min. Colorless block crystals of complex **1** were obtained in a yield of 37% (based on H_2FDC). Elemental anal. (%) calcd. for MnC$_6$H$_8$O$_8$: C 27.39 H 3.07; found: C 27.31 H 3.35. FTIR(KBr) $\tilde{\nu}$/cm^{-1}: 3341s 2359s 2342m 1581s 1551s 1418s 1370s 1222w 1039m 968m 845w 780m 669w 498w.

1.2.2 H_2N(CH$_3$)$_2$ $_2$· Mn$_3$(FDC)$_4$ · 2DMF · H_2O(**2**)

H_2FDC(0.0156 g 0.1 mmol) and MnCl$_2$ · 4H_2O(0.0198 g 0.1 mmol) were dissolved in DMF(2.0 mL) with stirring at room temperature. Then the solution was placed in a 10 mL conical flask. The container was heated to 100 ℃ at a rate of 5 ℃/min and kept at 100 ℃ for 24 h then slowly cooled down to room temperature at a rate of 3 ℃/min. Colorless needle crystals of complex **2** were obtained in a yield of 34% (based on H_2FDC). Elemental anal. (%) calcd. for Mn$_3$C$_{34}$H$_{40}$O$_{23}$N$_4$: C 39.32 H 3.86 N 5.40; found: C 39.13 H 3.79 N 5.13. FTIR(KBr) $\tilde{\nu}$/cm^{-1}: 3345s 2419w 1580s 1417s 1368s 1222w 1039m 968m 844m 780s 613m 498w.

1.3 X-Ray Crystallography

Data collections were performed on a Rigaku RAXIS-CS Imaging Plate at 298 K for complex **1** and performed on an Oxford Gemini S Ultra CCD area detector at 173 K for complex **2**. Absorption corrections were carried out using the analytical program Tompa-analytical for complex **1** and multiscan program CrysAlis Red for complex **2**. The structures were solved by the direct method and nonhydrogen atoms were refined anisotropically by least-squares on F^2 *via* the SHELXTL program [48]. The hydrogen atoms of organic ligands were

generated geometrically(C—H 0.096 nm; N—H 0.090 nm). Crystal data and the details of data collection and refinement are summarized in Table 1. CCDC reference numbers are 758944 and 758945.

Table 1   Crystallographic data for complexes 1 and 2

Complex	1	2			
Formula	$MnC_6H_8O_8$	$Mn_3C_{34}H_{40}O_{23}N_4$	T/K	298	173
F_w	263.06	1037.52	$D_{calcd.}/(g \cdot cm^{-3})$	1.860	1.660
Crystal system	Orthorhombic	Triclinic	μ/mm^{-1}	1.428	0.993
Space group	$Pnma$	$P\bar{1}$	Indep. refln.	1154	3633
a/nm	0.8180(2)	0.9449(2)	Absd. refln.	1010	2819
b/nm	0.7555(2)	1.0076(2)	Number of parameter	90	313
c/nm	1.5201(3)	1.1576(2)	Goodness of fit	1.204	1.035
$\alpha/(°)$	90	73.093(4)	R_{int}	0.0633	0.0302
$\beta/(°)$	90	89.597(4)	$R_1\ I>2\sigma(I)$	0.0744	0.0609
$\gamma/(°)$	90	80.097(4)	$wR_2\ I>2\sigma(I)$	0.2051	0.1792
V/nm^3	0.9394(3)	1.0378(2)	R_1(all data)	0.0791	0.0764
Z	4	1	wR_2(all data)	0.2076	0.1879

2   Results and Discussion

2.1   Description of Crystal Structures

Single-crystal structure analysis reveals that complex **1** crystallized in the orthorhombic system with space group $Pnma$ consists of one Mn^{2+} ion one FDC^{2-} ligand and three aqua ligands. As shown in Fig. 1(A) the independent Mn center is six-coordinated by one monodentate carboxylate one chelate carboxylate and three terminal aqua ligands displaying distorted octahedral coordination geometry. Each FDC^{2-} ligand connects two adjacent Mn^{2+} ions through its one carboxylate in chelating/bridging mode generating a one-dimensional chain as shown in Fig. 2.
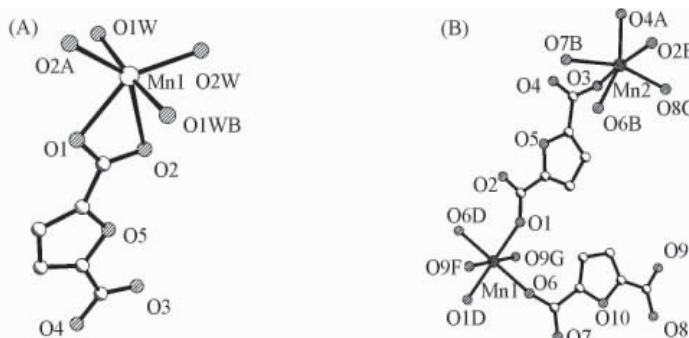

Fig. 1   ORTEP plot showing the coordination environment of Mn(Ⅱ) ion in complex 1(A) and the coordination environment of Mn(Ⅱ) ion in complex 2(B)

Symmetry codes: (A) A: $x+1/2$ y $-z+1/2$; B: x $-y+1/2$ z. (B) A: $-x$ $-y+2$ $-z$; B: $-x$ $-y+1$ $-z+1$; C: $-x+1$ $-y+1$ $-z+1$; D: $-x$ $-y$ $-z+1$; E: x $y+1$ z; F: $x-1$ y z; G: $-x+1$ $-y$ $-z+1$.

These 1D chains are further stacked into a 3D supramolecular architecture through hydrogen-bonding between the aqua ligands from one chain and the carboxylate oxygens from adjacent chains Fig. 3 $d(O1W—H1WA\cdots O4)=0.2773$ nm $d(H1WA\cdots O4)=0.1813$ nm $\angle O1W—H1WA\cdots O4=179.43°$ $\angle O1W—H1WB\cdots O3=0.2962$ nm $\angle H1WB\cdots O3=0.2002$ nm $\angle O1W—H1WB\cdots O3=179.62°$. The Mn—O distances are ranged from 0.2086(5) nm to 0.2554(5) nm compared to those of 0.2088(2)—0.2519(2) nm in the six-coordinated Mn(Ⅱ)-complex [49]. The distance of Mn$\cdots$Mn is 0.4395 nm which is similar to that of Mn$\cdots$Mn 0.4515 nm in carboxylate-bridged 1D Mn chain previously reported [50].

Complex **2** crystallized in $P\bar{1}$ group. Crystal structural analysis reveals that there are one and a half independent Mn^{2+} ions two FDC^{2-} ligands one DMF molecule half a water molecule and one $(CH_3)_2NH_2^+$ cation in the asymmetry unit of complex **2**. As shown in Fig. 1(B) Mn1 adopts an octahedral coordination
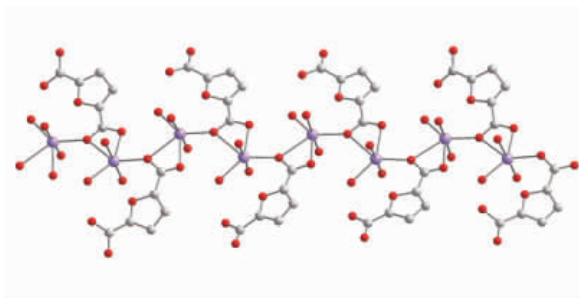
Fig. 2   Ball and stick view of 1D chain of complex 1

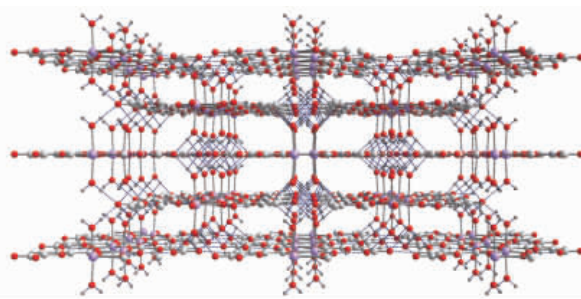Gray: C; violet: Mn; red: O. H atoms are omitted for clarity.

Fig. 3   Ball and stick view of 3D structure of complex 1 constructed by hydrogen‑bonding interactions

Gray: C; violet: Mn; red: O.

geometry constructed by six monodentate carboxylates from six different FDC^{2-} ligands while Mn2 locates in the center of a distorted octahedron geometry with four carboxylates in monodentate mode and one carboxylate in chelating mode respectively. The Mn—O distances are ranged from 0.2161(2) nm to 0.2355(2) nm compared to those of Mn—O 0.2142(2)—0.2253(3) nm in the six‑coordinated Mn(Ⅱ)‑complex [51]. The Mn1 center links two Mn2 centers through two carboxylates in *syn‑syn* bridging mode one carboxylate in chelating/bridging mode resulting in a Mn_3 unit. Connection of adjacent Mn_3 units through a pair of carboxylates in *syn‑anti* bridging mode generates a one‑dimensional chain along the *c*‑axis direction Fig. 4(A) . Such a 1D metallic chain is further linked to four chains through two types of FDC^{2-} ligands: one type of FDC^{2-} lig‑ ands with its one carboxylate in chelating/bridging mode and the other one in *syn‑syn* mode and the other type of FDC^{2-} ligands with its one carboxylate in *syn‑syn* mode and the other one in *syn‑anti* mode(Fig. 5) leading to a three‑dimensional open framework with 1D channels Fig. 4(B) . The channel along the *c* axis has a di‑ mension of 0.5991 nm × 0.6720 nm. The solvent‑accessible volume calculated through the PLATON program is approximately 0.461 nm^3 per unit cell volume(44.4%) [52]. The guest water molecules fill the void space
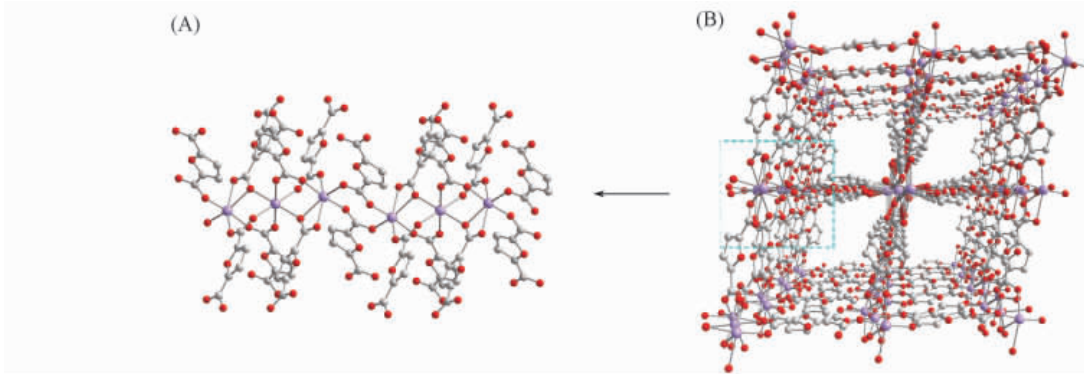

Fig. 4   Ball and stick view of the 1D chain in complex 2(A) and the 3D framework of complex 2(B)

Gray: C; violet: Mn; red: O. H atoms guest molecules and $(CH_3)_2NH_2^+$ cations are omitted for clarity.
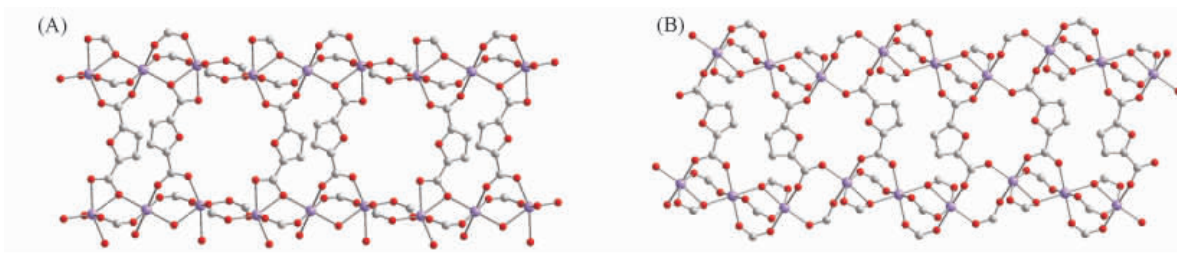

Fig. 5   1D metallic chain in complex 2 further linked to neighboring chains through two types of FDC^{2-} ligands

Gray: C; violet: Mn; red: O. H atoms are omitted for clarity.

while the $(CH_3)_2NH_2^+$ cations serve as guest molecules to balance the charges of the anionic framework. The distances of Mn···Mn are 0.3689 and 0.4751 nm for Mn1···Mn2 and Mn2···Mn2A respectively.

2.2 Influence of Solvent on the Structure of Complexes 1 and 2

Since the only difference in the synthetic condition between complexes **1** and **2** is that of the reaction sol−vent it is clear that reaction solvent plays a key role in controlling the structures of the complexes. Reaction of $MnCl_2 \cdot 4H_2O$ and H_2FDC in DMF solvent produces a 3D open framework whereas a 1D chain is formed when the reaction carried out in DMF/H_2O solvent. On the basis of the structures of complexes **1** and **2** two Mn centers are entirety coordinated by six and five FDC^{2-} ligands in complex **2** whereas three water molecules and two FDC^{2-} ligands coordinate to the Mn centers in complex **1**. The introduction of the auxiliary terminal ligands water molecules not only adjusts the coordination environments of the Mn centers but also restricts the 1D chains expanding into 2D or 3D framework resulting in the structure of complex **1** being significantly distinct from that of complex **2**.

2.3 Thermal Stability

The TGA analysis indicates that complex **1** is stable up to 140 ℃ and then has two steps of mass loss (Fig. 6). The first mass loss of 20.6% from 140 ℃ to 190 ℃ corresponds to the loss of the coordinated water molecules(calcd. 20.5%). No further mass loss was observed between 190 and 340 ℃ indicating that over this temperature range the composition of the dehydrated product remains unchanged. The second step from 340 ℃ to 390 ℃ is attributed to the further decomposition of the FDC^{2-} ligand. The TG analysis of complex **2** shows the first mass loss of 14.5% between 100 ℃ and 175 ℃ which is attributed to the loss of water molecules and DMF molecules(calcd. 15.8%). When the temperature is higher than 175 ℃ the $(CH_3)_2NH_2^+$ ions begin to be lost followed by the de−composition of complex **2** to lose the organic ligands.
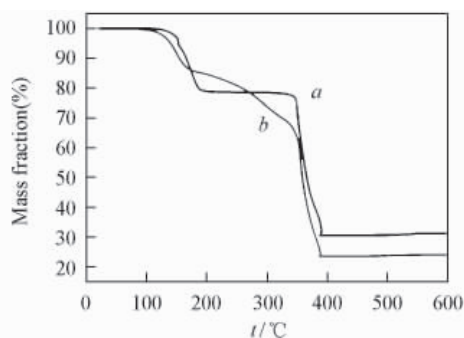
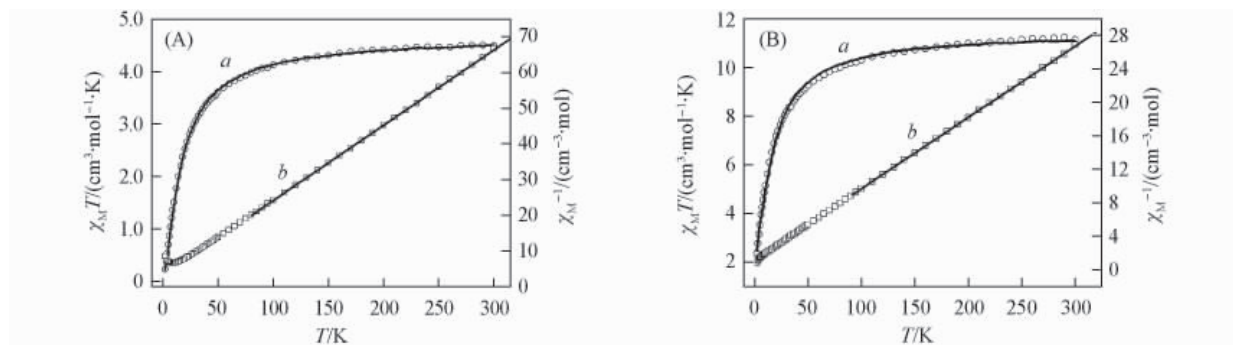**Fig.6** TG analysis curves of complexes 1(*a*) and 2(*b*)

Fig.7 Plots of $\chi_M T$ vs. $T(a)$ and χ_M^{-1} vs. $T(b)$ for complexes 1(A) and 2(B)

2.4 Magnetic Properties

The magnetic properties of complexes **1** and **2** were investigated through variable−temperature susceptibili−ty measurement in a temperature range of 2 K to 300 K with an applied magnetic field of 7.96×10^4 A/m. The resulting $\chi_M T$ vs. T and χ_M^{-1} vs. T plots for complexes **1** and **2** are given in Fig.7(A) and (B) respectively. The $\chi_M T$ value of complex **1** at room temperature is 4.50 cm^3·mol^{-1}·K(300 K) consistent with the value ex−pected for one independent Mn^{2+} ion following a Curie law with $g = 2.03$. Upon lowering the temperature the value of $\chi_M T$ decreases gradually down to 50 K and then decreases abruptly to 2 K with a minimum value of 0.24 cm^3·mol^{-1}·K. The χ_M^{-1} data in a range of 100—300 K were fitted to Curie−Weiss law $\chi(T) = C/(T - $

θ) with a Curie constant of $C = 4.73$ cm^3·mol^{-1}·K and a Weiss constant of $\theta = -14.29$ K indicating antiferromagnetic coupling between two Mn(Ⅱ) atoms through μ_2: η^1 η^2-carboxylate bridge.

Similar to complex **1** complex **2** also shows the varieties of the $\chi_M T$ vs. T and χ_M^{-1} vs. T plots. The $\chi_M T$ value of complex **2** at room temperature is 11.14 cm^3·mol^{-1}·K(300 K) corresponding to the value of three independent Mn^{2+} ions($g = 1.85$). The $\chi_M T$ value decreases slowly until 50 K. After that it drops rapidly to 2.37 cm^3·mol^{-1}·K at 2 K. The Curie constant of $C = 11.74$ cm^3·mol^{-1}·K and Weiss constant of $\theta = -13.86$ K exhibit antiferromagnetic coupling between two Mn^{2+} ions via μ_2: η^1 η^2-carboxylate and two syn-syn 1 3-μ_2-carboxylate bridge.

In order to investigate the magnetic properties of complexes **1** and **2** Quantum Monte Carlo(QMC) simu-lation QMC simulation was performed by the SSE [53 54] and the loop algorithm [55] based on the project of ALPS (Algorithms and Libraries for Physical Simulations) [56]. For each site 1×10^6 Monte Carlo steps were per-formed and 10% of them were discarded as the initial transient stage. The sample included 300 spins which is large enough to prevent finite size effects was carried out based on the corresponding Hamiltonian as shown in Eqs. (1) and (2). QMC methods are emerging as a powerful tool for analysizing the magnetic data of low-dimensional systems with quantum spins [57-64].

$$H = -J_1 \sum S_i S_{i+1} \tag{1}$$

$$H = -J_1 \sum (S_{3i+1} S_{3i+2} + S_{3i+2} S_{3i+3}) - J_2 \sum S_{3i} S_{3i+1} \tag{2}$$

Inspection of the 1D Mn chain in complexes **1** and **2** there are one exchange parameter in complex **1** and two exchange parameters in complex **2** as shown in Fig. 8. The best simulated parameters are $J_1 = -3.1$ cm^{-1} $g = 2.07$ and $R = 7.17 \times 10^{-5}$ for complex **1**; $J_1 = -3.5$ cm^{-1} $J_2 = -0.3$ cm^{-1} $g = 1.87$ and $R = 1.48 \times 10^{-4}$ for complex **2** where R is calculated from $\sum (\chi_M)_{obs.} - (\chi_M)_{calcd.}^2 / \sum (\chi_M)_{obs.}^2$. The lit-tle negative J values imply weak antiferromagnetic interaction propagated through carboxylate groups in com-plexes **1** and **2** which are consistent with those in other manganese complexes with similar bridge ligands [65]. The lower g value in complex **2** ($g = 1.87$) is similar to those in other Mn clusters previously reported with g values of 1.87 and 1.89 [66]. Both the complexes have the similar 1D chains in which each Mn^{2+} ion linked by the carboxylate groups exhibits the similar magnetic behavior. Particularly the two carboxylate groups with syn-syn mode in complex **2** reinforce the antiferromagnetic interaction $J_1(\mathbf{2}) < J_1(\mathbf{1})$. Furthermore Mn2···Mn2A in complex **2** is bridged by two carboxylate groups in syn-anti mode also producing weak antiferromag-netic interaction($J_2 = -0.3$ cm^{-1}).
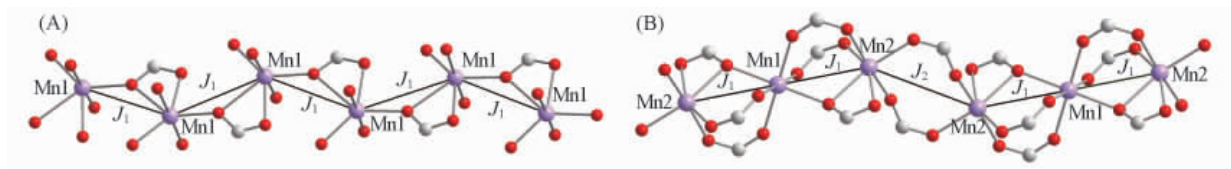

Fig. 8   Magnetic exchange scheme used for complexes 1(A) and 2(B)
Gray: C; violet: Mn; red: O.

3   Conclusions

In summary we have successfully synthesized two coordination polymers through the solvothermal reaction of MnCl$_2$·4H$_2$O and H$_2$FDC under different solvent conditions. Investigation on their structural differences reveals that the coordination environment of the metal centers is affected by the coordination ability of the solvent molecules giving the control of the structures of these complexes. Variable-temperature magnet-ic measurements and Quantum Monte Carlo(QMC) simulation indicate that both the complexes exhibit antifer-romagnetic characteristic.

References

1　Dong Y. B.　Wang P.　Ma J. P.　Zhao X. X.　Wang H. Y.　Tang B.　Huang R. Q.. J. Am. Chem. Soc. J　2007 **129**(16)： 4872—4873

2　Wang P.　Ma J. P.　Dong Y. B.　Huang R. Q.. J. Am. Chem. Soc. J　2007 **129**(35)： 10620—10621

3　Tang S. F.　Song J. L.　Li X. L.　Mao J. G.. Cryst. Growth Des. J　2007 **7**(2)： 360—366

4　Chen B.　Wang L.　Zapata F.　Qian G.　Lobkovsky E. B.. J. Am. Chem. Soc. J　2008 **130**(21)： 6718—6719

5　Yamamoto C.　Nishikawa H.　Nihei M.　Shiga T.　Hedo M.　Uwatoko Y.　Sawa H.　Kitagawa H.　Taguchi Y.　Iwasa Y.　Oshio H.. Inorg. Chem. J　2006 **45**(25)： 10270—10276

6　Zhang W.　Xiong R. G.　Huang S. D.. J. Am. Chem. Soc. J　2008 **130**(32)： 10468—10469

7　Fu D. W.　Ye H. Y.　Ye Q.　Pan K. J.　Xiong R. G.. Dalton Trans. J　2008： 874—877

8　Clérac R.　Miyasaka H.　Yamashita M.　Coulon C.. J. Am. Chem. Soc. J　2002 **124**(43)： 12837—12844

9　Bai Y. L.　Tao J.　Wernsdorfer W.　Sato O.　Huang R. B.　Zheng L. S.. J. Am. Chem. Soc. J　2006 **128**(51)： 16428—16429

10　Zheng Y. Z.　Tong M. L.　Zhang W. X.　Chen X. M.. Angew. Chem. Int. Ed. J　2006 **45**(38)： 6310—6314

11　Xu H. B.　Wang B. W.　Pan F.　Wang Z. M.　Gao S.. Angew. Chem. Int. Ed. J　2007 **46**(39)： 7388—7392

12　Seo J. S.　Whang D.　Lee H.　Jun S. I.　Oh J.　Jeon Y. J.　Kim K.. Nature J　2000 **404**(6781)： 982—986

13　Zhao X.　Xiao B.　Fletcher A. J.　Thomas K. M.　Bradshaw D.　Rosseinsky M. J.. Science J　2004 **306**(5698)： 1012—1015

14　Lin X.　Jia J.　Zhao X.　Thomas K. M.　Blake A. J.　Walker G. S.　Champness N. R.　Hubberstey P.　Schröder M.. Angew. Chem. Int. Ed. J　2006 **45**(44)： 7358—7364

15　Humphrey S. M.　Chang J. S.　Jhung S. H.　Yoon J. W.　Wood P. T.. Angew. Chem. Int. Ed. J　2007 **46**(1/2)： 272—275

16　Banerjee R.　Phan A.　Wang B.　Knobler C.　Furukawa H.　O'Keeffe M.　Yaghi O. M.. Science J　2008 **319**(5865)： 939—943

17　Rather B.　Zaworotko M. J.. Chem. Commun. J　2003： 830—831

18　Dybtsev D. N.　Chun H.　Kim K.. Angew. Chem. Int. Ed. J　2004 **43**(38)： 5033—5036

19　Zheng S. L.　Yang J. H.　Yu X. L.　Chen X. M.　Wong W. T.. Inorg. Chem. J　2004 **43**(2)： 830—838

20　Zhang J. P.　Lin Y. Y.　Huang X. C.　Chen X. M.. Chem. Commun. J　2005： 1258—1260

21　Forster P. M.　Burbank A. R.　Livage C.　Férey G.　Cheetham A. K.. Chem. Commun. J　2004： 368—369

22　Tong M. L.　Kitagawa S.　Chang H. C.　Ohba M.. Chem. Commun. J　2004： 418—419

23　Zhang J.　Bu X. H.. Chem. Commun. J　2008： 444—446

24　Dalgarno S. J.　Hardie M. J.　Raston C. L.. Cryst. Growth Des. J　2004 **4**(2)： 227—234

25　Zheng P. Q.　Ren Y. P.　Long L. S.　Huang R. B.　Zheng L. S.. Inorg. Chem. J　2005 **44**(5)： 1190—1192

26　Zhang G.　Yang G.　Ma J. S.. Cryst. Growth Des. J　2006 **6**(2)： 375—381

27　Bauer S.　Bein T.　Stock N.. Inorg. Chem. J　2005 **44**(16)： 5882—5889

28　Ghosh S. K.　Kitagawa S.. Cryst. Eng. Comm. J　2008 **10**(12)： 1739—1742

29　Shi C. Y.　Ge C. H.　Gao E. J.　Yin H. X.　Liu Q. T.. Inorg. Chem. Commun. J　2008 **11**(6)： 703—706

30　Forster P. M.　Stock N.　Cheetham A. K.. Angew. Chem. Int. Ed. J　2005 **44**(46)： 7608—7611

31　Go Y. B.　Wang X.　Anokhina E. V.　Jacobson A. J.. Inorg. Chem. J　2005 **44**(23)： 8265—8271

32　Fang R. Q.　Zhang X. M.. Inorg. Chem. J　2006 **45**(12)： 4801—4810

33　Zhou Z. H.　Deng Y. F.　Wan H. L.. Cryst. Growth Des. J　2005 **5**(3)： 1109—1117

34　Zhou Y. F.　Lou B. Y.　Yuan D. Q.　Xu Y. Q.　Jiang F. L.　Hong M. C.. Inorg. Chim. Acta J　2005 **358**(11)： 3057—3064

35　Chen W. X.　Wu S. T.　Long L. S.　Huang R. B.　Zheng L. S.. Cryst. Growth Des. J　2007 **7**(6)： 1171—1175

36　Wu S. T.　Long L. S.　Huang R. B.　Zheng L. S.. Cryst. Growth Des. J　2007 **7**(9)： 1746—1752

37　Yu F.　Kong X. J.　Zheng Y. Y.　Ren Y. P.　Long L. S.　Huang R. B.　Zheng L. S.. Dalton Trans. J　2009： 9503—9509

38　Chen B.　Fronczek F. R.　Maverick A. W.. Chem. Commun. J　2003： 2166—2167

39　Pedireddi V. R.　Varughese S.. Inorg. Chem. J　2004 **43**(2)： 450—457

40　Wu T.　Li D.　Ng S. W.. Cryst. Eng. Comm. J　2005 **7**(84)： 514—518

41　Yang J.　Li G. D.　Cao J. J.　Yue Q.　Li G. H.　Chen J. S.. Chem. Eur. J. J　2007 **13**(11)： 3248—3261

42　Wang F. K.　Yang S. Y.　Huang R. B.　Zheng L. S.　Batten S. R.. Cryst. Eng. Comm. J　2008 **10**(9)： 1211—1215

43　Yuan H. B.　Yang S. Y.　Xie Z. X.　Huang R. B.　Batten S. R.. Inorg. Chem. Commun. J　2009 **12**(8)： 755—757

44　Felloni M.　Blake A. J.　Hubberstey P.　Wilson C.　Schröder M.. Cryst. Growth Des. J　2009 **9**(11)： 4685—4699

45　Kim Y. J.　Lee E. W.　Jung D. Y.. Chem. Mater. J　2001 **13**(8)： 2684—2690

46　Cañada-Vilalta C.　Streib W. E.　Huffman J. C.　O'Brien T. A.　Davidson E. R.　Christou G.. Inorg. Chem. J　2004 **43**(1)：

101—115

47 Jia H. P.   Li W.   Ju Z. F.   Zhang J. . Chem. Commun. J   2008: 371—373

48 SHELXTL 6. 10. CP   Madison: Bruker Analytical Instrumentation   2000

49 Kim D. S.   Forster P. M.   Delgado G. D.   Parkc S. E.   Cheetham A. K. . Dalton. Trans. J   2004: 3365—3369

50 Albela B.   Corbella M.   Ribas J.   Castro I.   Sletten J.   Stoeckli-Evans H. . Inorg. Chem. J   1998 **37**(4): 788—798

51 Rzaczynska Z.   Bartyzel A.   Glowiak T. . Polyhedron J   2003 **22**: 2595—2599

52 Spek A. L. . Acta Crystallogr. Sect. A: Found. Crystallogr. J   1990 **46**: C34

53 Sandvik A. W.   Kurkijarvi J. . Phys. Rev. B J   1991 **43**(7): 5950—5961

54 Sandvik A. W. . J. Phys. A: Math. Gen. J   1992 **25**(13): 3667—3682

55 Sandvik A. W. . Phys. Rev. B J   1999 **59**(22): R14157—R14160

56 Alet F.   Dayal P.   Grzesik A.   Honecker A.   Koerner M.   Laeuchli A.   Manmana S. R.   McCulloch I. P.   Michel F.   Noack R. M.   Schmid G.   Schollwoeck U.   Stoeckli F.   Todo S.   Trebst S.   Troyer M.   Werner P.   Wessel S. . J. Phys. Soc. Jpn. Suppl. J   2005 **74**: 30—35

57 Yamamoto S. . J. Phys. Soc. Jpn. J   1994 **63**(12): 4327—4330

58 Yamamoto S.   Hori H. . Phys. Rev. B J   2005 **72**(5): 054423—054428

59 Murtazaev A. K.   Magomedov M. A. . J. Magn. Magn. Mater. J   2006 **300**(1): e570—e573

60 Mennerich C.   Klauss H. H.   Brökelmann M.   Litterst F. J.   Golze C.   Klingeler R.   Kataev V.   Büchner B.   Grossjohann S. N.   Brenig W.   Goiran M.   Rakoto H.   Broto J. M.   Kataeva O.   Price D. J. . Phys. Rev. B J   2006 **73**(17): 174415—174422

61 Demeshko S.   Leibeling G.   Dechert S.   Fuchs S.   Pruschke T.   Meyer F. . Chem. Phys. Chem. J   2007 **8**(3): 405—417

62 Tangoulis V.   Panagoulis D.   Raptopoulouc C. P.   Dendrinou-Samara C. . Dalton Trans. J   2008: 1752—1760

63 Nie F. M.   Demeshko S.   Fuchs S.   Dechert S.   Pruschke T.   Meyer F. . Dalton Trans. J   2008: 3971—3977

64 Bai Y. L.   Tangoulis V.   Huang R. B.   Zheng L. S.   Tao J. . Chem. Eur. J. J   2009 **15**(10): 2377—2383

65 Kim Y. J.   Lee E. W.   Jung D. Y. . Chem. Mater. J   2001 **13**(8): 2684—2690

66 Wittick L. M.   Jones L. F.   Jensen P.   Moubaraki B.   Spiccia L.   Berry K. J.   Murray K. S. . Dalton. Trans. J   2006: 1534—1543

(Ed.: V   N)